JOURNAL OF APPLIED ELECTROCHEMISTRY 3 (1973) 91–98

Field crystallization of anodic films on tantalum

N. F. JACKSON

Allen Clark Research Centre, Towcester, Northants., U.K.

Received 18 September 1972

The radial growth rate of crystalline areas during the anodization of tantalum is found to be related to the nature and concentration of both the solute and the solvent and also to the pH of the electrolyte. In general, the use of high solute concentrations or the addition of certain organic solvents produces reduced growth rates in aqueous electrolytes.

Structural examinations indicate that for bright rolled tantalum foil of nominal purity 99·99%, the density of nucleation sites is approximately 10^7 cm^{-2}, of which about 1% undergo active radial growth. The nucleation sites, which can be related to impurity inclusions, are believed to maintain contact with the electrolyte through narrow pores. As the amorphous oxide is rolled back by the growing crystals, a layer of relatively uniform thickness is stripped from the top surface of the crystalline area and remains in intimate contact with the detached amorphous oxide.

The use of field crystallization to study the location and distribution of impurities at both exterior and interior surfaces of sintered powder anodes is described.

1. Introduction

The major electrical breakdown effects of thin oxide films on tantalum during anodization are scintillation and field crystallization. Scintillation is a catastrophic effect which produces widespread physical damage and often leads to the development of a short circuit. On the other hand, field crystallization is a more gradual process leading to a progressive deterioration of the dielectric properties. Crystalline oxide is a product of both processes but the way in which the crystalline areas are formed is quite different. When scintillation occurs, the heat developed by the spark discharge leads to thermal transformation of the amorphous film. In the case of field crystallization, the amorphous film is displaced by a crystalline phase which grows by anodization.

Field crystallization was first described by Vermilyea [1, 2] who suggested that the growth of the crystalline material took place in two stages. Initially, amorphous oxide was transformed into crystalline oxide at the nucleation site. Stresses created by density differences in the two materials produced cracks in the amorphous film. Once contact with the electrolyte was established through the crack, crystalline growth continued by anodization. Vermilyea also showed that in hot dilute nitric acid solution the logarithm of incubation time (defined as the elapsed time to the first appearance of nuclei) was inversely proportional to the electric field strength across the amorphous oxide (constant temperature) and inversely proportional to temperature (constant field strength across amorphous oxide).

The purpose of the present paper is to show how the growth of the crystalline areas is controlled by selection or modification of the electrolyte composition. New structural data are presented and the implications of these results on the growth process are discussed.

2. General Description

When degreased tantalum foil is anodized in hot nitric acid solution, a current versus time relationship of the form shown in Fig. 1 is observed.

The left hand portion of the curve in the region of minimum current (t_{min}) results from the interaction of two separate processes. At $t<t_{min}$, the current is dominated by the formation of amorphous oxide and at $t>t_{min}$ by the formation of crystalline oxide, both processes passing essentially equal currents at t_{min}. The value of t_{min} increases (and the attendant current decreases) as the voltage and temperature of anodization are reduced and the purity of the metal is increased. Following t_{min} the current rises, passes through a maximum and then decreases. Observations of the electrolytic cell in a dark chamber indicate that the anode emits visible radiation in the region of the maximum current.

For a specimen showing a current-voltage plot similar to Fig. 1, a number of small cracks

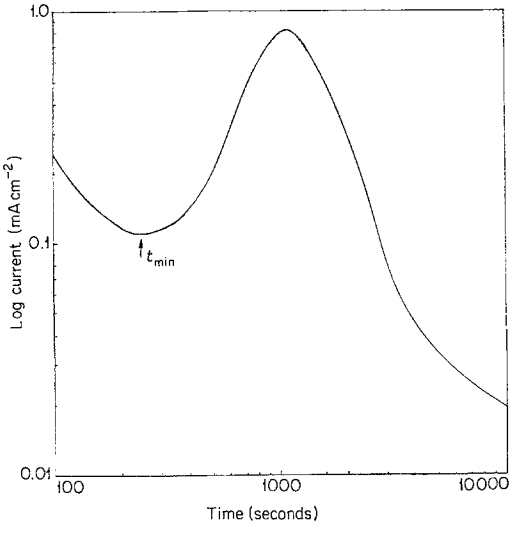

Fig. 1. Leakage current versus time relationship during anodization in 2% HNO_3 at 110 V, 100°C.

(approximately 1–2 μm in size) can be observed at the surface after a few minutes' polarization (Fig. 2a). The cracks are produced by crystalline nuclei forming within the amorphous oxide. With increasing anodization time, the crystalline areas grow outwards radially, at the same time pushing back the amorphous film (Fig. 2b–d). The crystalline areas possess fairly regular polygonal shapes which may be easily identified with an optical microscope. As the diameters of the polygons increase, contact with neighbouring crystals is established; at this stage the current reaches a maximum value. Subsequently, the current decreases and the process is concluded when essentially all the amorphous oxide has been displaced. The final thickness of the crystalline film is substantially greater than that of the amorphous oxide. Electrical measurements indicate that the capacitance is approximately halved and both the dissipation factor and the leakage current show considerable increases.

Vermilyea established that the surface of each crystalline area consisted of a number of small crystals elongated in the radial direction. The crystals were arranged in segments and within individual segments all the crystals were parallel and at right angles to the boundary. The sectors were most easily observed by examining the surface with polarized light.

Of the two parameters, namely voltage and temperature, which control the growth of the crystalline phase in any particular electrolyte, temperature has the dominant influence. Consequently, it is usually possible to minimize crystallization by reducing the temperature and increasing the voltage. This effect is illustrated in Fig. 3 for films anodized to the same thickness. The application of this result is most important in relation to niobium, because radial growth rates on this metal are much higher than with tantalum. Thick films essentially free of crystals can only be produced on niobium by anodizing at low temperatures.

3. Parameters Controlling Radial Growth

3.1. *Experimental*

The majority of this work was conducted with bright-rolled tantalum foil of thickness 0·0025 cm. The nominal purity was 99·99%, spectrographic analysis indicating the major impurity to be iron with a concentration of 10 ppm. Smaller quantities of copper, aluminium and calcium were also present. Prior to anodizing, the foil was degreased by treatment with warm methyl ethyl ketone.

The tantalum was anodized either by direct application of the forming voltage (constant voltage) or by polarization at a constant current density of 2 mA cm^{-2} to a predetermined level and then changing to constant voltage (constant

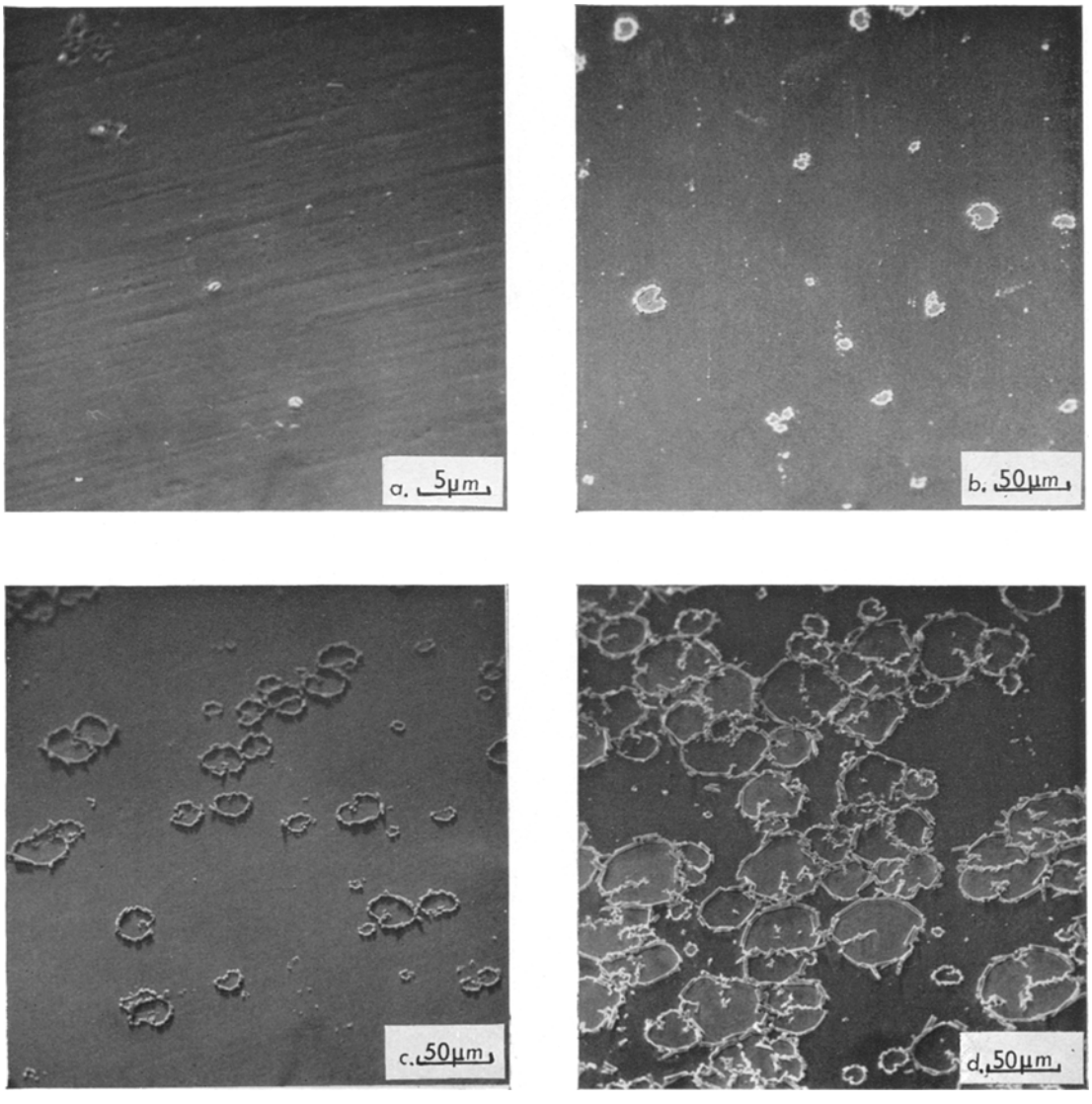

Fig. 2. Crystalline areas formed during anodization in 2% HNO_3 at 120 V, 85°C: (a) 5 min, (b) 16 min, (c) 30 min, (d) 90 min.

facing p. 92

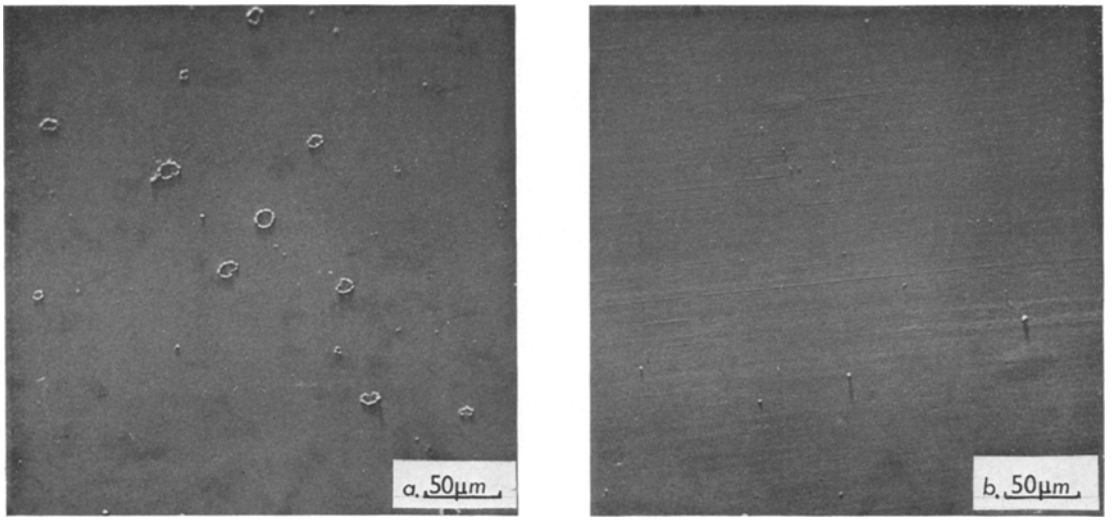

Fig. 3. Crystalline areas formed after anodization in 2% HNO_3 to the amorphous oxide thickness of 1650 Å: (a) 82 V, 85°C, 90 min, (b) 100 V, 20°C, 90 min.

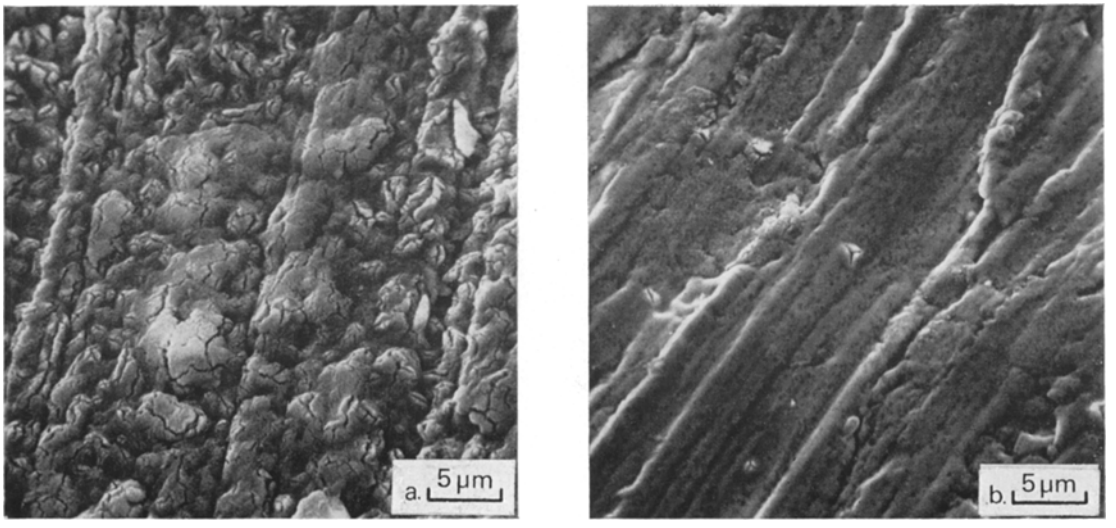

Fig. 4. Anodized tantalum plate: (a) as received, (b) after pickling.

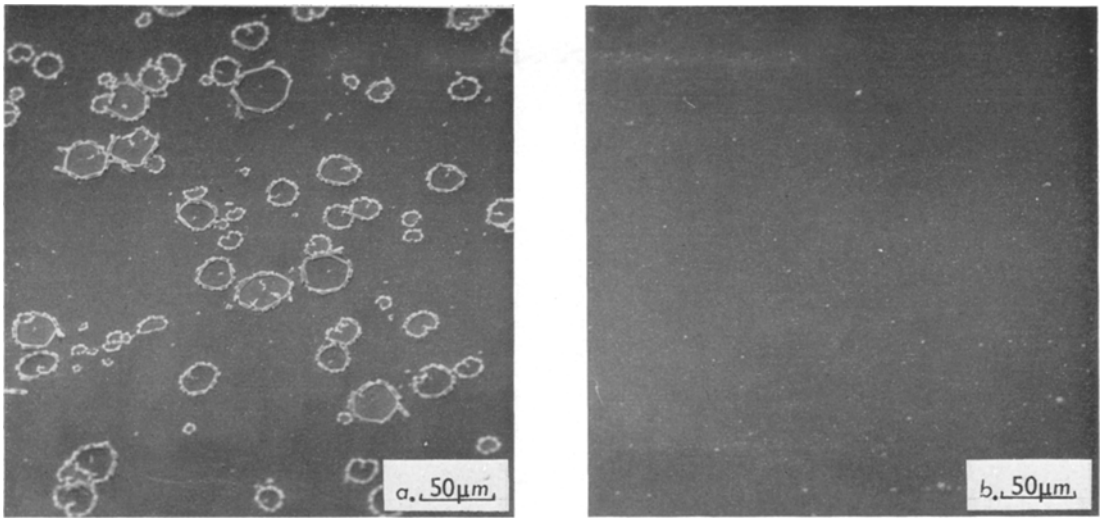

Fig. 5. Degree of crystallization after anodizing in H_2SO_4 electrolytes at 100 V, 85°C, 90 min: (a) 0·2% H_2SO_4, (b) 10% H_2SO_4.

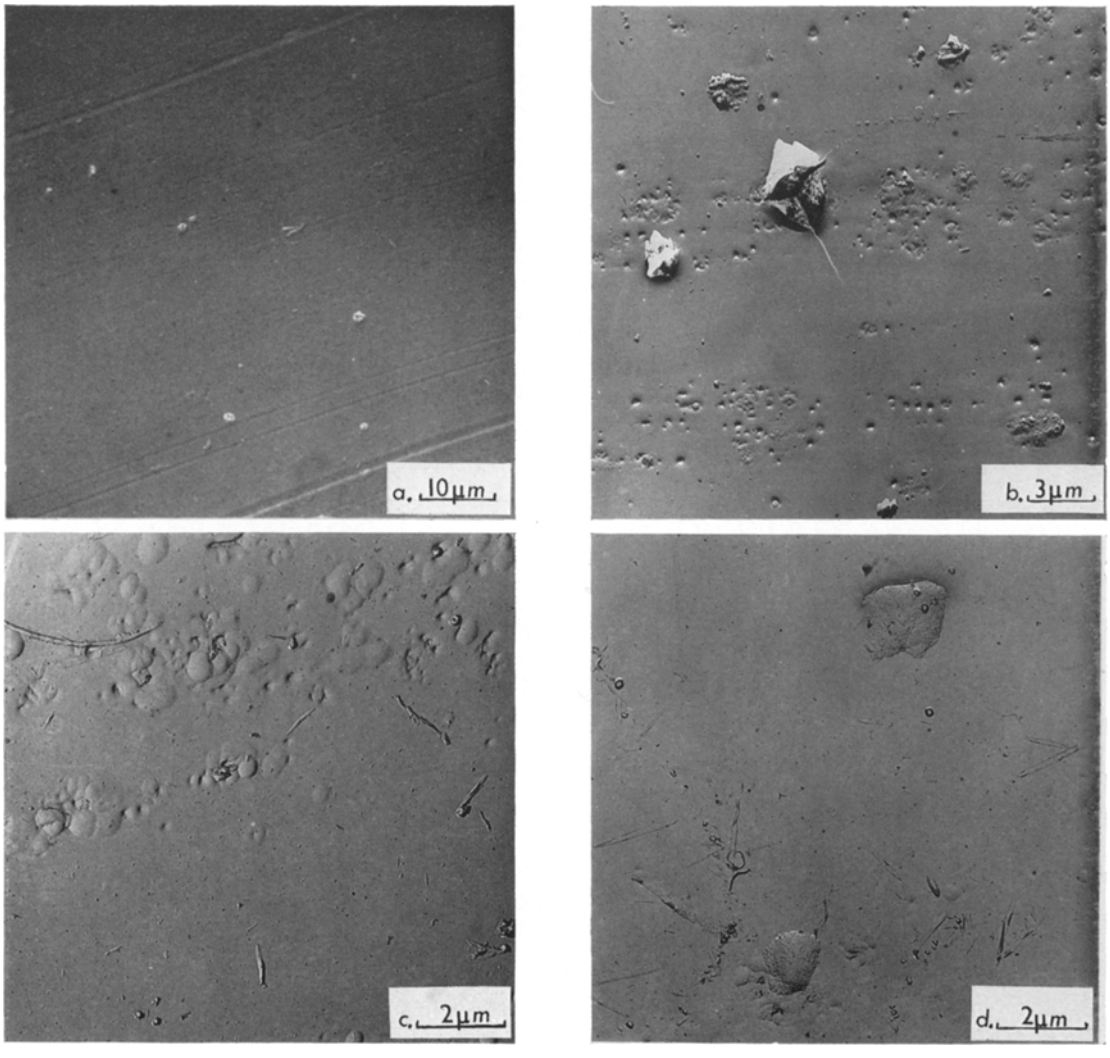

Fig. 6. Anodized in 1% H_3PO_4 at 150 V, 85°C, 60 min: (a) and (b) oxide-air interface, (c) and (d) oxide-metal interface.

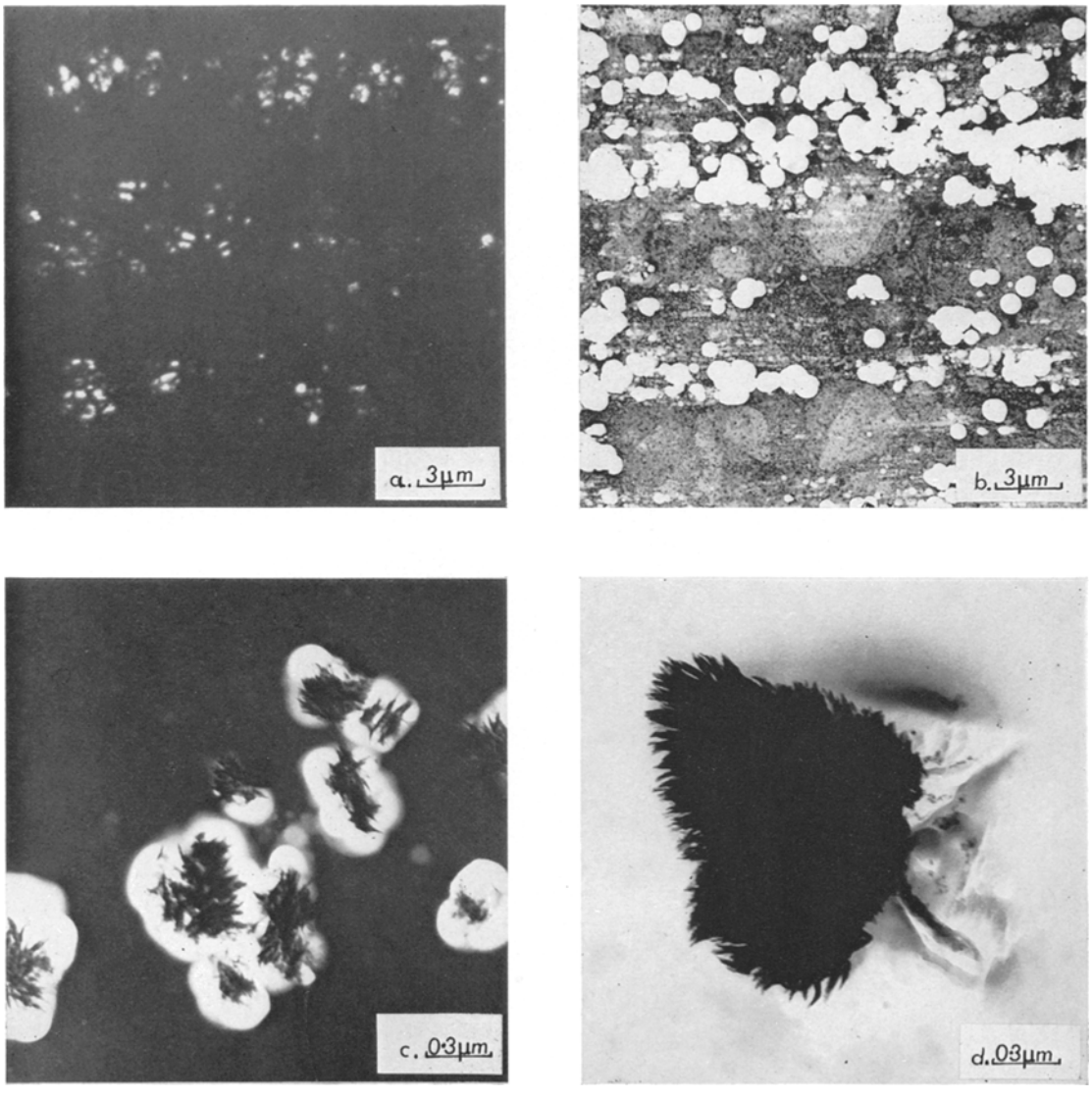

Fig. 8. Anodized in 1% H_3PO_4 at 150 V, 85°C, 60 min: (a) transmission micrograph of stripped oxide, (b) as (a) thinned to half thickness, (c) as (a) slightly thinned, (d) extraction replica of oxide-air interface.

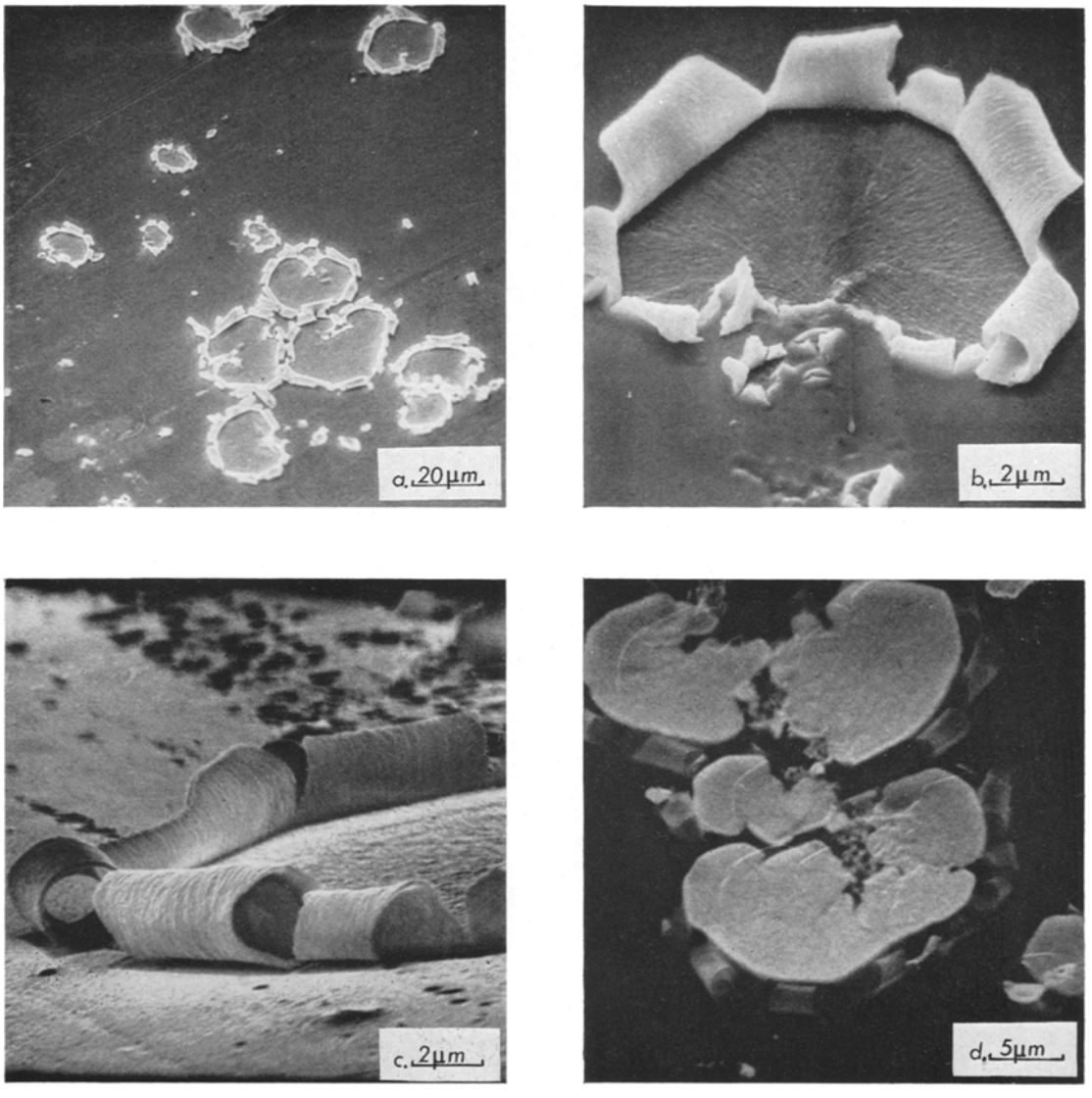

Fig. 9. Anodized in 2% HNO_3 at 120 V, 85°C, 16 min: (a) and (b) oxide-air interface, (c) as (a) amorphous oxide dissolved, (d) extraction replica of oxide-metal interface.

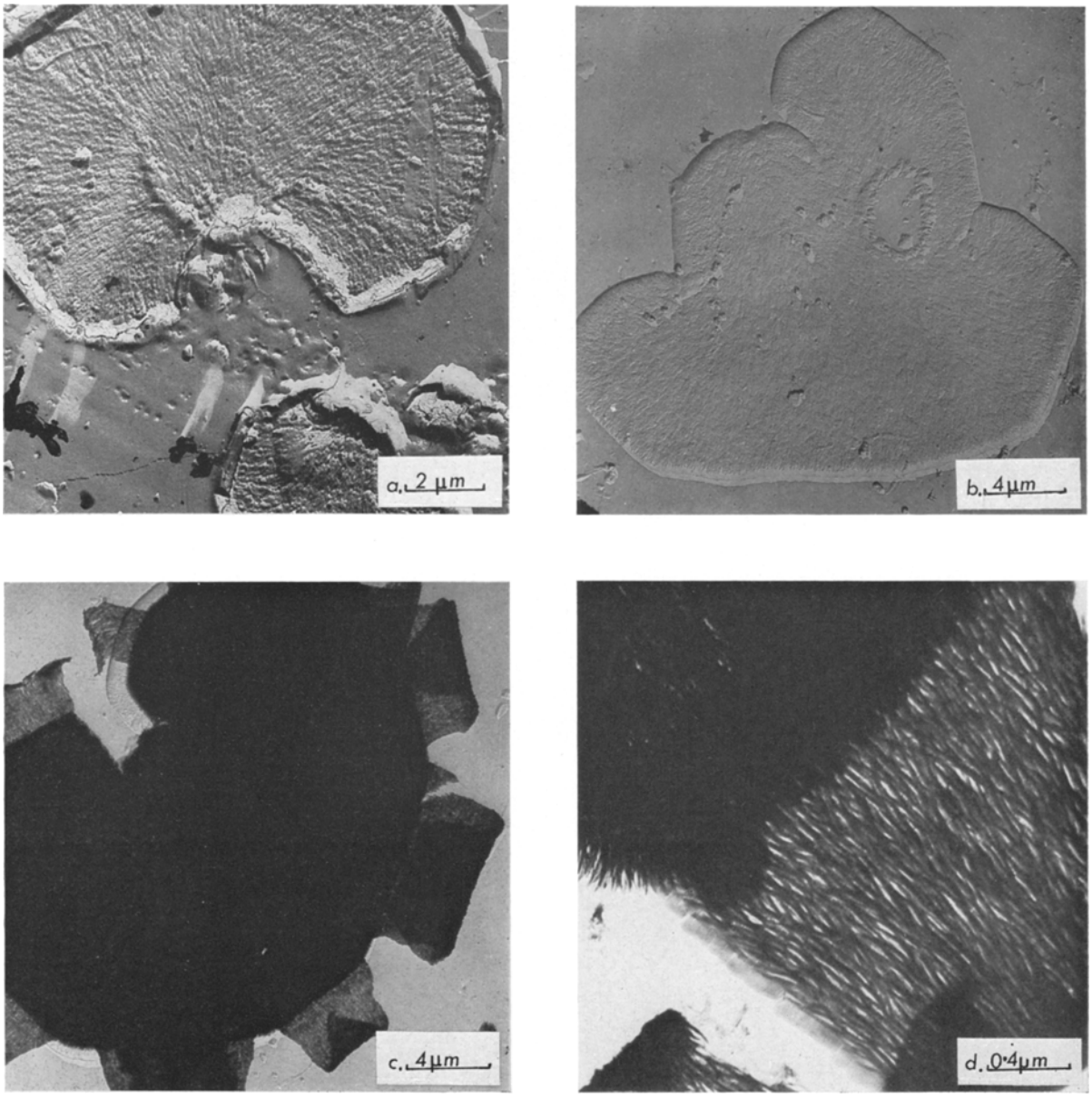

Fig. 11. Anodization in 2% HNO_3 at 120 V, 85°C, 16 min: (a) oxide-metal interface, (b) metal-oxide interface, (c) and (d) extraction replicas of metal-oxide interface.

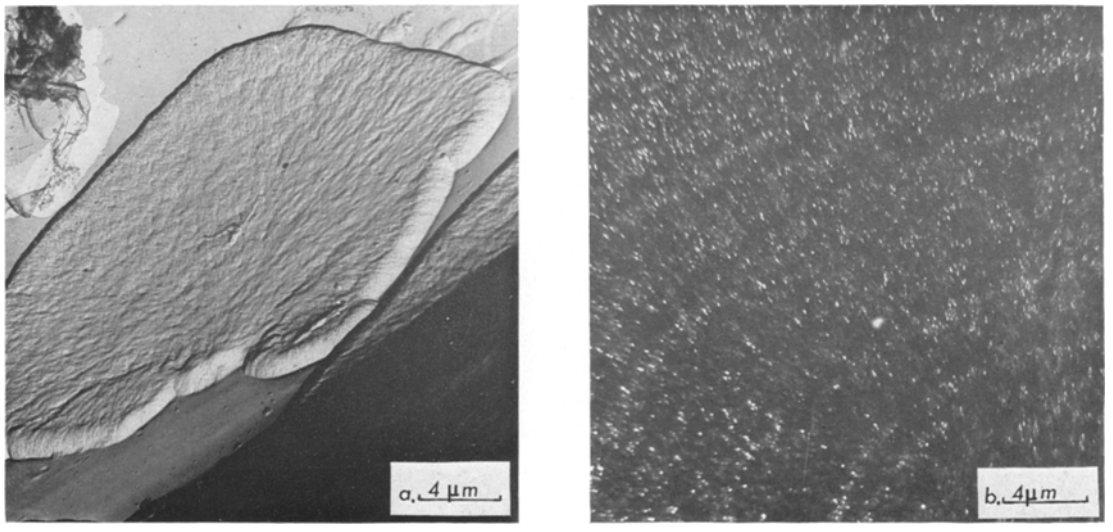

Fig. 12. Anodized in 2% HNO_3 at 85°C: (a) 16 min anodization, oxide-metal interface, (b) 30 min anodization, transmission through stripped oxide showing porosity.

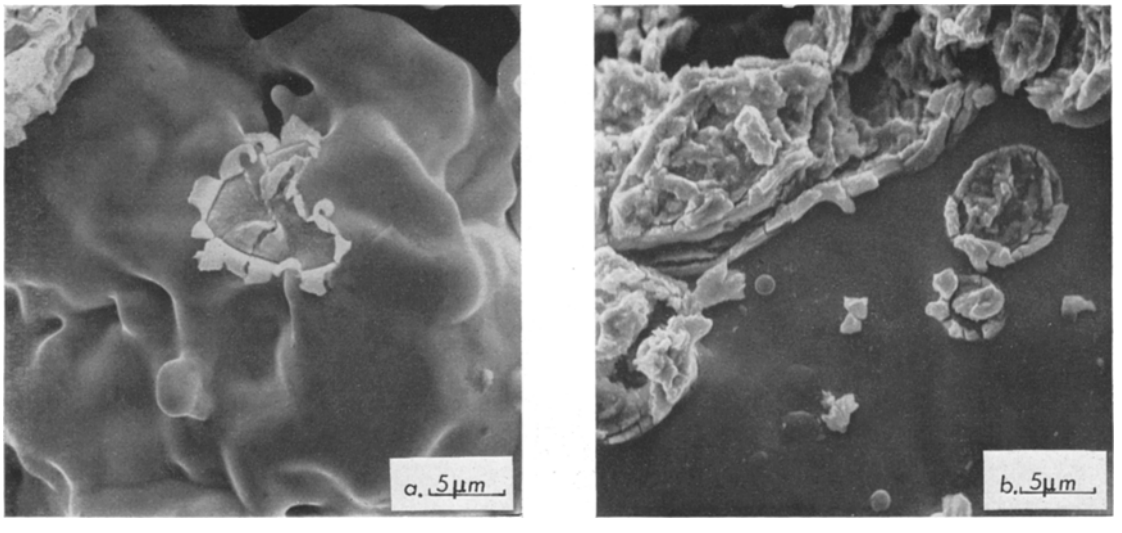

Fig. 14. Radial growth of crystalline areas on porous anodes: (a) HNO_3 anodization, (b) from capacitor after 8000 h storage at 150 V, 85°C.

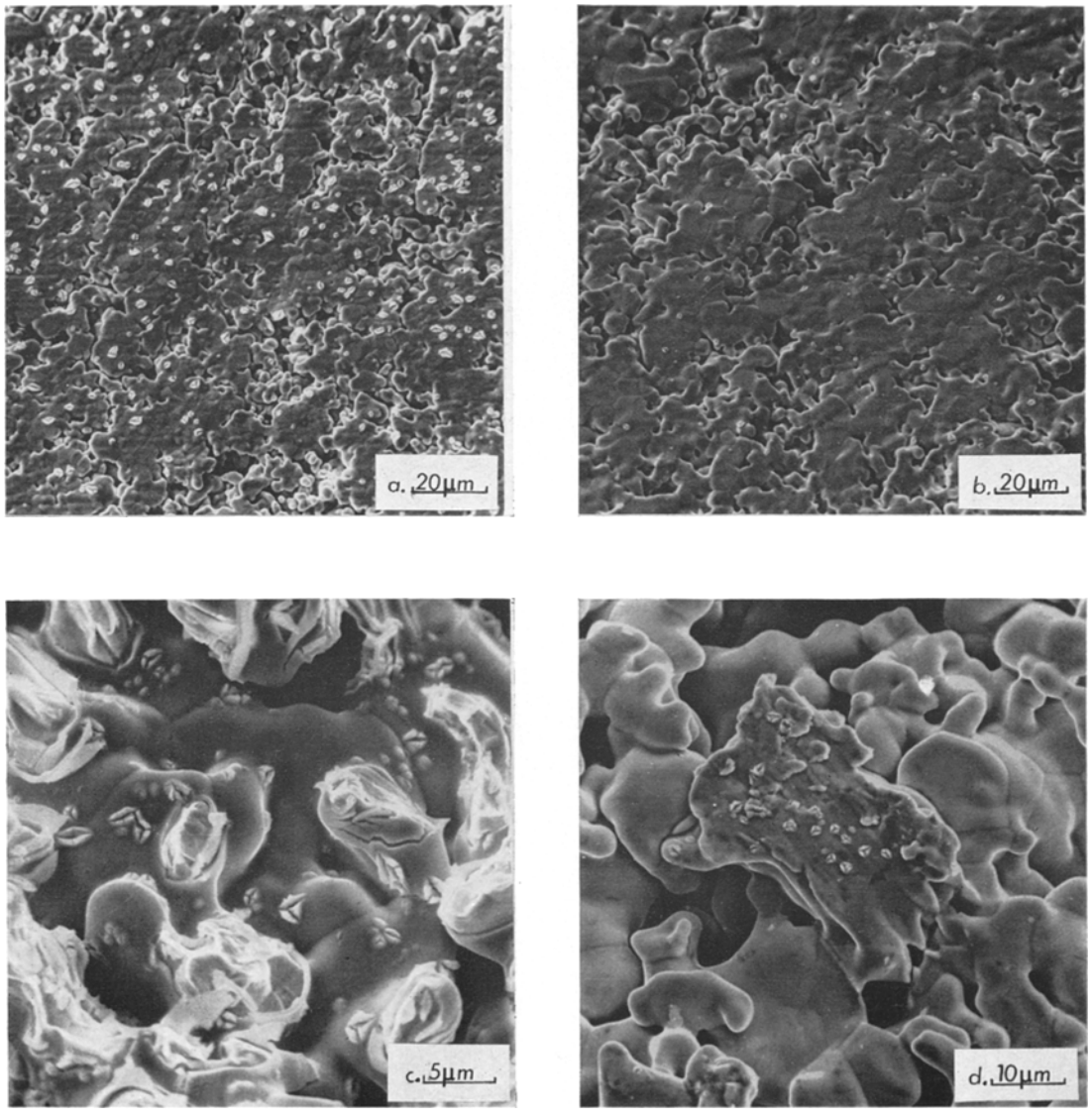

Fig. 13. Crystalline areas on anodized sintered bodies: (a) sintered at 1600°C, (b) sintered at 1900°C, (c) section, binder contamination, (d) anodes in contact in sintering crucible.

facing p. 93

current/voltage). In the latter case, the indicated time of anodization refers to the time after reaching constant voltage.

In some experiments the degree of crystallization was determined by measuring the relative area of crystalline to amorphous oxide at the metal surface. For these measurements an optical microscope at a magnification of ×200 was employed.

3.2. *Metal purity*

Surface purity rather than bulk purity is the principal factor governing the number of crystalline areas. Since the surface of tantalum foil or plate is often heavily contaminated by the rolling process, electropolishing or chemical pickling has a considerable influence on field crystallization (Fig. 4). Laboratory experiments indicated that mechanical strains introduced into the surface by scratching with a tantalum wire had no observable effect on crystallization. On the other hand, scratching with iron, copper, silver or zinc led to a major increase in the number of crystalline areas. Valve metals, e.g. niobium or aluminium, or electrolytically discharged hydrogen produced no effect.

3.3. *Influence of electrolyte*

3.3.1. *Composition and pH.* An approximate guide to the radial growth rate was achieved by determining t_{min} in the current versus time plot. The results for a number of different electrolytes after polarization at a constant voltage of 110 V for periods of not less than 60 min are given in Table 1.

The absence of a t_{min} value in these experiments is indicative of a low radial growth rate. It is apparent that a high growth rate is generally associated with an electrolyte of low pH and a low growth rate with an electrolyte of high pH. Of the acid solutions, phosphoric acid was exceptional and behaved much like an alkaline system. The results also suggest that there is an effect related to the specific nature of the solute as well as to pH.

The effect of pH was examined in more detail by anodizing at constant voltage in a range of oxalic acid–sodium oxalate mixtures. The degree of crystallization as a function of pH is given in Table 2.

At pH values below 4·8 almost the whole of the surface was covered with crystalline oxide. In a solution of pH 5·2, the response was variable. Although most of the surface showed widespread crystallization, some areas showing a reduced growth rate were observed. A sharp decrease in the amount of crystalline film occurred at pH 5·6 and with increasing pH above this value the proportion of crystalline oxide decreased. However, the differences in oxalate

Table 1. Values of t_{min} for tantalum specimens anodized at 110 V in electrolytes of 2% concentration at 100°C

Electrolyte composition (20g l^{-1})	*Electrolyte pH at 20°C*	*Electrolyte conductivity (Ω^{-1} cm^{-1})*	t_{min} (min)
HNO_3	0·6	0·11	5
H_2SO_4	0·7	0·088	22
$(COOH)_2$	1·0	0·036	27
H_3PO_4	1·2	0·015	Not observed
CH_3COOH	2·4	0·00087	10
$K_2Cr_2O_7$	3·8	0·014	33
NaCl	5·4	0·030	27
Na_2SO_4	6·0	0·018	23
CH_3COONa	8·2	0·011	Not observed
$Na_2B_4O_7$	9·5	0·010	Not observed
$(COONa)_2$	9·7	0·011	Not observed
Na_2CO_3	11·1	0·024	Not observed
NaOH	13·3	0·048	Anode scintillated

Table 2. Degree of crystallization for tantalum specimens anodized at 110 V for 240 min in oxalic acid–sodium oxalate solutions of uniform conductivity (0·020 Ω^{-1} cm^{-1} at 20° C)

Electrolyte pH at 20°C	*Electrolyte composition (% w/v)*		*Crystalline area (%)*
	Oxalic acid	*Sodium oxalate*	
1·2	0·9	0·0	>90
3·8	0·4	2·6	>90
4·8	0·04	2·1	>90
5·2	0·02	2·0	(>90)
5·6	<0·01	2·0	9·0
6·9	<0·01	2·0	1·3
8·3	<0·01	2·0	0·9
9·7	No addition	2·0	0·6

ion concentration for all pH values from 4·8 upwards were small.

3.3.2. *Concentration.* Tantalum specimens were anodized by the constant current/voltage method in sulphuric acid electrolytes of different concentration for 90 min. The degree of field crystallization and the size and frequency of crystalline areas at the surface of the specimens are listed in Table 3. Because of the limitation in the magnification, it was not possible to include in this analysis crystalline areas below $2{\cdot}5 \times 10^{-5}$ mm^2 in size. While this factor has a very small effect on the amount of crystalline material formed, many small nuclei cannot be included in the frequency count. In consequence, frequency is given in Table 3 in terms of the number of visible areas.

Table 3. Degree of crystallization for tantalum specimens anodized in sulphuric acid electrolytes at 100 V and 85°C for 90 min

Sulphuric acid concentration (% w/v)	*Crystalline area (%)*	*Number of visible crystalline areas (10^4 cm^{-2})*	*Average size of crystalline areas (10^{-5} mm^2)*
0·2	11·5	4·6	17
2·0	1·2	1·9	4
10·0	<0·1	—	—
49·0	<0·1	—	—

As the concentration increased from 0·2% to 2·0% the proportion of crystalline film at the surface decreased; at 10% and 49% no crystallization was observed. The number of crystals and also their average size decreased with increasing concentration. Scanning electron micrographs of specimens formed in 0·2% and 10% electrolyte are shown in Fig. 5. The 49% solution is identical to the 40% w/w electrolyte that is often employed in commercial electrolytic capacitors.

Qualitatively similar results were obtained with oxalic acid and sodium sulphate electrolytes. However, nitric acid gave an anomalous result and, at least in the concentration range 0·2% to 2·0%, showed an increase in crystallization with increasing concentration.

3.3.3. *Organic solvents.* The influence of organic solvents was assessed by anodizing by the constant current/voltage technique in 2% oxalic acid solutions containing various amounts of ethylene glycol. The results for additions of 0 to 5% by volume of glycol are given in Table 4.

Table 4. Degree of crystallization for tantalum specimens anodized in 2% oxalic acid–glycol–water electrolyte at 120 V and 85°C for 90 min

Ethylene glycol addition (Vol.%)	*Crystalline area (%)*	*Number of visible crystalline areas (10^4 cm^{-2})*	*Average size of crystalline areas (10^{-5} mm^2)*
0	5·7	3·7	9
1	0·7	1·7	~2
5	0·2	—	—

For glycol concentrations of 10, 25 and 50 and 75 volume %, the crystalline areas covered <0·1% of the surface. These results indicate that quite small concentrations of glycol can produce large changes in the radial growth rate. Other work involving solutions of sulphuric acid in amyl alcohol and glycerol has confirmed this general effect of organic solvents.

3.3.4. *Radial growth rates.* It is well established that small quantities of the forming electrolyte are incorporated in the oxide film [3]. However, experiments in which tantalum was preformed in a range of different electrolytes, including phosphoric acid and alcoholic solutions, did not indicate that the subsequent growth rate in nitric acid was significantly altered. Therefore, it can be assumed that the influence of incorporated impurities is either very small or negligible.

Advantage can be taken of this result to measure radial growth rates in a variety of different electrolytes. Specimens were anodized for 40 min at a constant voltage of 110 V in 2% nitric acid at 100°C. A suitable site was selected with the optical microscope and the diameters of a number of relatively large crystalline areas (approximately 30 μm in size) were measured in two directions at right angles. The foils were then further anodized in the test electrolyte at the same voltage and temperature for a convenient

period prior to re-measurement. Under these conditions the second anodization was performed under essentially constant electric field conditions across the amorphous oxide. Results obtained with 0·5% sodium sulphate electrolytes containing various additions are given in Table 5.

Table 5. Radial growth rate of crystalline areas anodized in 0·5% sodium sulphate electrolytes at 110 V and 100°C (field strength = 0·041 VÅ^{-1})

Additive to 0·5% sodium sulphate electrolyte (% w/v)	*Radial growth rate (Å sec^{-1})*
None	150
1·0% Thiourea	150
1·0% Sodium flouride	140
0·1% Boric acid	140
1·0% Gelatine	110
0·1% Cetyl trimethyl ammonium bromide	100
1·0% 8-Hydroxy quinoline	80
0·16% Ammonium hydrogen arsenate	10
0·1% Phosphoric acid	0·65

Most surface active agents led to some reduction in growth rate. The most dramatic effects were achieved with ammonium hydrogen arsenate and phosphoric acid. In practice, growth rates were found to be essentially uniform for crystalline areas varying in diameter from 20 to 70 μm. However, when the growth rate was severely reduced, further growth was irregular indicating that inhibition was not entirely uniform around the polygonal boundary.

4. Structure

4.1. *Specimen preparation*

Structural work was performed after anodization either in phosphoric acid (low radial growth rate) or nitric acid (high radial growth rate). Specimens for examination in the scanning electron microscope were coated with a palladium–gold alloy to minimize charging effects. For studies with the transmission microscope, replicas were prepared by coating with platinum–carbon and subsequently detaching by treating the specimen with hydrofluoric acid–nitric acid. For transmission work or replication of the lower surface, the anodic film was stripped from the metal by immersion in bromine–methanol. When extraction replicas were employed, the stripped film was coated on one surface with platinum–carbon and then treated in hydrofluoric acid for the minimum time required to dissolve the amorphous component.

4.2. *Phosphoric acid anodization*

Tantalum specimens were anodized using the constant current/voltage technique at 150 V in 1% phosphoric acid at 85°C for 60 min. Micrographs of the oxide–air and the oxide–metal interfaces are shown in Fig. 6.

A general view of the oxide–metal interface (Fig. 6a) showed the presence of a number of surface cracks having a population density of approximately 10^5 cm^{-2}. Very little radial growth had occurred. At rather higher magnification (Fig. 6b) the linear structure of the rolling damage was resolved into a large number of small surface indentations (~0·2 μm in diameter), suggesting a marked degree of porosity. Two crystallization cracks as well as some areas of general surface roughness were also apparent. On the underside of the oxide (Fig. 6c) the features characteristic of rolling damage took two forms. The first was a raised dome, indicating that excess metal had reacted in these regions. The second was an indentation suggesting that some of the pores passed completely through the oxide film. However, many of the open pores at the metal interface had ridges around the circumference. The way these twin features can be related to the size and positioning of impurities is illustrated schematically in Fig. 7. In other regions of the oxide–metal interface (Fig. 6d) a number of fibrous structures were observed; these were evidently the undersides of relatively large crystalline areas which had produced cracks in the upper surface.

Transmission microscopy of stripped films confirmed the presence of pores passing through the oxide (Fig. 8a). On thinning the film to approximately half its initial thickness prior to examination, the pores opened out into circular

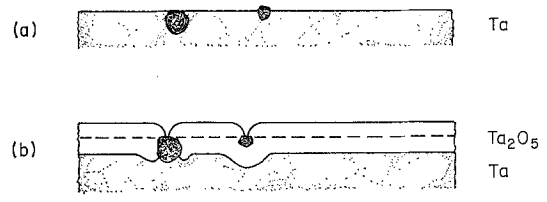

Fig. 7. Schematic diagram of pore formation: (a) before anodizing, (b) after anodizing.

holes of about 1 μm diameter (Fig. 8b). In both micrographs the relationship to rolling damage is clearly recognizable. If the film was only slightly thinned (Fig. 8c), it was found that many of the holes retained small crystalline clusters, approximately 0·15–0·3 μm in diameter and having a population density in the region of 10^7 cm^{-2}. Each cluster appeared to be composed of fibres or rods of length about 1500Å and width 30Å. Selected area electron diffraction indicated the presence of monoclinic β-Ta_2O_5 of crystallite size 50–250Å. An extraction replica from the upper surface of the stripped film showed the replica of a crack and the well-developed crystal producing it (Fig. 8d).

4.3. *Nitric acid anodization*

Samples were anodized by the constant current/voltage technique at 120 V in 2% nitric acid at 85°C for 16 min.

Scanning electron micrographs (Fig. 9a) of the surface indicated a relatively wide distribution in size of the crystalline areas, from 1 μm up to about 40 μm. However, the number of sites was similar to that observed in the phosphoric acid anodization, i.e. approximately 10^5 cm^{-2}. At higher magnification, the striated nature of the underside of the rolled-back film and the relationship of this feature to the structure of the main crystalline area was apparent (Fig. 9b). On treating specimens with hydrofluoric acid to dissolve the amorphous oxide, it was found that not all of the detached film had dissolved (Fig. 9c). Closer examination indicated that a thin layer at the underside, i.e. the surface originally adjoining the crystalline area, was essentially insoluble. An extraction replica taken from the under-surface of stripped film, examined with the crystalline fraction uppermost, confirmed the presence of thin cylinders attached to the boundaries of the crystalline areas (Fig. 9d). These observations suggest that as the amorphous coating is peeled back by the growing crystals, a thin layer of crystalline film at the interface becomes detached and remains in intimate contact with the amorphous oxide. A schematic diagram illustrating this mechanism is shown in Fig. 10. The thickness measurements given, which pertain to a 60 min polarization in 2% nitric acid at 120 V, were taken from sections examined with the scanning electron microscope.

Replication of the oxide–air interface was made after lightly brushing the surface to remove displaced film. Examination with the transmission microscope revealed in more detail the fibrous nature of the crystalline areas and the orientation of the fibres with respect to the boundary (Fig. 11a). The undersurface showed a similar structure but generally this interface was considerably smoother (Fig. 11b), presumably because of the absence of peeling. The extraction replicas of Fig. 11c and d disclosed the fibrous structure of the oxide attached to the boundary of the main crystalline areas. Selected area electron diffraction indicated that the material of these filaments was identical to that of the micro-crystallites found in the phosphoric acid formed oxide (Fig. 8c).

The larger crystalline areas were found to be essentially of uniform thickness, except at the edges, and all showed a marked penetration into the metal surface (Fig. 12a). In transmission, the fibrous structure was prominent and a degree of porosity was also apparent (Fig. 12b).

5. Sintered Powder Anodes

The majority of tantalum electrolytic capacitors, both liquid filled and solid electrolyte types, employ sintered powder rather than foil anodes. The sintered bodies retain a high degree of porosity and possess large surface areas. The sintering, which is applied in vacuum at temperatures in the region of 1800–2100°C, produces a substantial degree of purification. The higher the temperature the greater is the purification, but there is an accompanying increase in densification and a reduction in surface area. A compromise must be reached between these opposing requirements, and powders are under con-

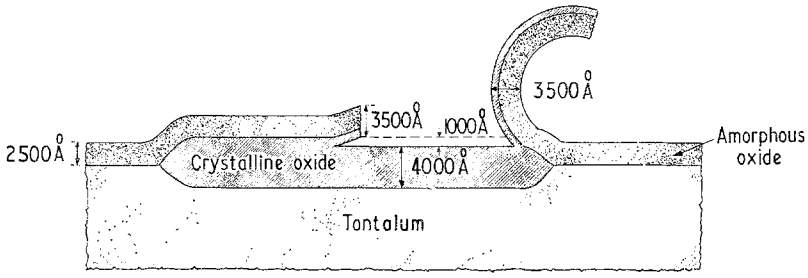

Fig. 10. Schematic digram of crystalline growth. Thicknesses relate to anodization in 2% HNO_3 at 120 V, 85°C, 60 min.

tinuing study in order to achieve the optimum properties.

The purity of the exposed surface of the porous anodes plays a controlling role in determining the performance and life of a capacitor. For this reason, bulk analysis has not proved uniquely helpful in selecting suitable powders. However, breakdown effects like field crystallization which are promoted by impurities, provide a useful method for studying anode surfaces. Unlike scintillation, the relatively mild breakdown phenomena produced by field crystallization enable the location and distribution of impurities to be determined with some precision.

An example of the influence of sintering temperature on purity is illustrated in Fig. 13a, b. In general it is found that the inner surfaces of the anodes are free of crystallization, although some centres can be observed at low sintering temperatures. This leads to the view that the organic binding agents, which are used to press the powders in the green state, normally have little effect on surface purity. However, the binders have to be chosen with care and dewaxing must be done under controlled conditions. The very high degree of crystallization shown in the section (Fig. 13c) has been caused by an experimental binder. On the basis of these observations it is concluded that the use of presses employing iron die-walls can contribute significantly to the contamination of the outer surface of porous anodes. A related problem arises when adjacent anodes stick together during sintering. On breaking apart on removal from the chamber, the contact surface is found to have undergone little purification and considerable crystallization occurs in this area (Fig. 13d).

When considerable radial growth occurs on the surface of a porous anode, e.g. when anodized in nitric acid, the crystalline area is sometimes found to be cracked. It seems that the peeled back amorphous film does not always succeed in completely detaching the top surface of the crystalline oxide on these anodes. An example of this is shown in Fig. 14a. Another unusual feature has been observed with experimental high voltage capacitors stored for long periods with a voltage applied. Examination of the leakage current versus time characteristic showed a distinctive t_{min} value followed by a fairly uniform rate of current increase (Fig. 15). After 8000 h of application of the voltage the crystalline regions were found to protrude prominently above the surface of the amorphous oxide and to show very irregular growth (Fig. 14b). It seems probable that, because of their porous nature, no true limiting thickness is reached with the crystalline films, but that they continue to grow in the vertical direction for a considerable time. In these circumstances, severe cracking of the film may take place.

6. Discussion

The relationship between impurity inclusions in the metal surface and field crystallization is well established. The results from the present work indicate that the amorphous oxide does not cover the nucleation sites and that electrolytic contact to the impurity is maintained through a narrow pore. The reason for the persistence of the pore has not been examined but it is probable that most of the electrolytic path is blocked by gas formation. There is no evidence that pores are

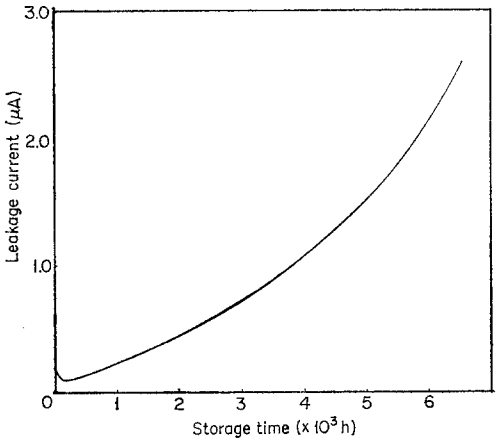

Fig. 15. Leakage current of tantalum capacitor during storage at 85°C with 150 V applied.

self-destroying, as argued by Vermilyea. Accepting that at least a tenuous electrolytic path is maintained to the nucleation site, it is evident that anodization will control the growth process from an early stage and not only after the crystals have grown to such a size that a crack is produced in the amorphous film. However, many of the small crystalline growths within the amorphous film do not undergo appreciable radial growth. The structural work suggests that this situation may largely result from the isolation of these crystals from the metal surface, thereby minimizing anodic growth.

The growth rate of the crystalline areas increases as the voltage and temperature of anodization is increased. Under conditions of constant voltage and temperature, the rate is controlled by the composition, concentration and pH of the electrolyte. The way in which the electrolyte influences growth is not understood. It is assumed that specific adsorption occurs at the edges of the crystalline oxide and that this has an inhibiting effect upon the electrochemical reaction. The quite general effect of increased concentration producing a reduction in the growth rate is in harmony with this proposition. However, the increased rate observed with more concentrated nitric acid presents an anomalous situation which requires further study.

Recent work, not yet completed, suggests that the growth rate at constant field strength and constant temperature is voltage dependent and not thickness dependent. This result is consistent with the observed influence of voltage under normal anodizing conditions, i.e. a reducing field strength, but appears to be in conflict with Vermilyea's work which showed that incubation time was field but not thickness dependent.

The crystalline areas appear quite rapidly to reach a relatively uniform thickness, which is substantially greater than that of the amorphous oxide. The latter effect is probably related to the smaller activation energy required for ionic movement in the crystalline oxide; in glassy materials, there will be a much greater tendency for ions to take part in bonding. Examination of specimens polarized for very long periods suggests that thickening may continue but at a relatively low rate. This feature is probably associated with the observed porosity of the crystalline areas.

7. Conclusions

1. The radial growth rate of crystalline oxide during anodization at constant voltage and temperature is controlled by the electrolyte.
2. The electrolyte maintains contact with the nucleation centres through narrow pores.
3. Only a small proportion of the nuclei undergo active radial growth.
4. The crystalline oxide has a fibrous structure and grows to a greater thickness than the amorphous oxide.

Acknowledgements

The author would like to thank Mr N. S. Griffin for the scanning electron micrographs and Mr P. Shaw for the transmission electron micrographs. This work is published by permission of The Plessey Company Limited.

References

[1] D. A. Vermilyea, *J. Electrochem. Soc.*, **102** (1955) 207.
[2] D. A. Vermilyea, *J. Electrochem. Soc.*, **104** (1957) 542.
[3] J. J. Randall, Jr., W. J. Bernard and R. R. Wilkinson, *Electrochimica Acta*, **10** (1965) 183.